

The Phase Diagram of Two Color QCD

Simon Hands¹, Seamus Cotter², Pietro Giudice¹ and
Jon-Ivar Skullerud²

¹ Physics Department, College of Science, Swansea University, Singleton Park,
Swansea SA2 8PP, UK

² Department of Mathematical Physics, National University of Ireland Maynooth,
Maynooth, County Kildare, Ireland

E-mail: `s.hands@swan.ac.uk`

Abstract. I present recent results from lattice simulations of SU(2) gauge theory with $N_f = 2$ Wilson quark flavors, at non-zero quark chemical potential μ . The thermodynamic equation of state is discussed along with the nature of the high density matter which forms. It is conjectured that deconfinement may mean different things for bulk and Fermi surface phenomena.

1. Why Two Colors?

In this talk I will give an update on our project to simulate SU(2) gauge theory with $N_f = 2$ quark flavors on cold lattices with quark chemical potential $\mu \neq 0$ [1, 2, 3]. Because of the Sign Problem, QC₂D offers currently the best prospect of using lattice simulations to study gauge theories at non-zero baryon charge density. In particular, we can explore the systematics of the lattice approach in this unexplored physical regime. There is good news: unlike the case of hot QCD, it is possible to perform a scan in μ at fixed cutoff, and the primary thermodynamic observable, the quark number density $n_q \equiv -\partial f / \partial \mu$, as a component of a conserved current has no quantum corrections. The bad news is that both UV and IR artifacts are significant and complicated; only recently have we begun to make progress in disentangling them [3].

A second, more theoretical motivation is that QC₂D with $\mu \neq 0$ offers the chance to explore color deconfinement in a new physical régime, complementary to the more usually studied transition at $T > 0$. There are interesting differences which will challenge us to refine the language used to discuss this essential feature of non-abelian gauge theories.

2. The Simulation

We define our lattice theory with the Wilson plaquette action and unimproved Wilson fermions with hopping parameter κ . Chemical potential is introduced via the standard prescription of weighting forward/backward temporal hops by $e^{\pm \mu a}$. Reality of the fermion measure follows from $\det M = \det \tau_2 M^* \tau_2$ where the Pauli matrix τ_2 acts on color. Our only innovation [1] is the introduction of a scalar, isoscalar and gauge-invariant diquark source term $jqq \equiv j\kappa(\psi_2^{tr} C\gamma_5\tau_2\psi_1 - \bar{\psi}_1 C\gamma_5\tau_2\bar{\psi}_2^{tr})$, where subscripts denote flavor. Setting $j \neq 0$ mitigates the IR fluctuations due to Goldstone modes associated with superfluidity at non-zero quark density. Indeed, j is nothing but a Majorana mass for the quarks. Fig. 1 shows how the computational effort, measured by both the number of `congrad` iterations and the HMC timestep dt required

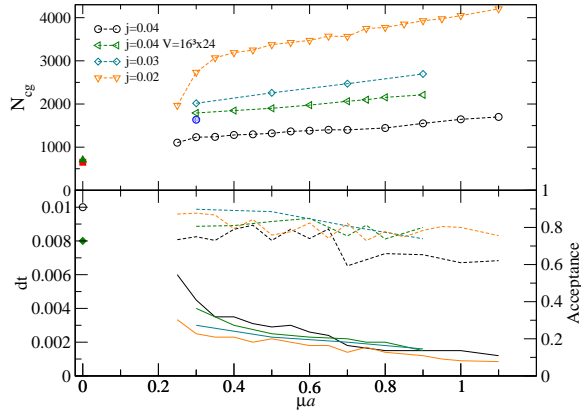


Figure 1. Computational effort needed for QC₂D.

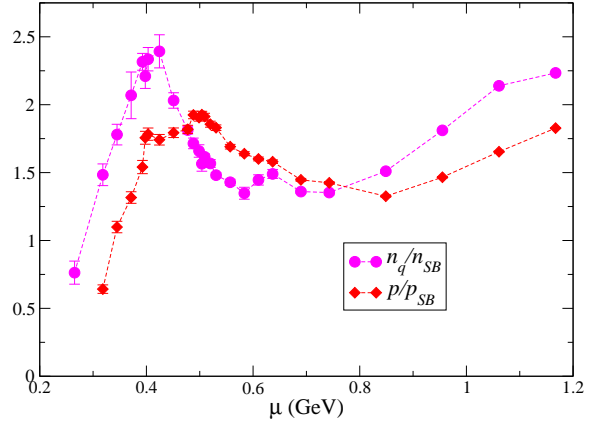


Figure 2. n_q/n_q^{SB} and p/p^{SB} for $ja = 0.04$ on $12^3 \times 24$.

for decent acceptance varies with μ and j . Despite the absence of a Sign Problem, studies of dense matter still require an order of magnitude more cpu than that needed for vacuum QCD.

By now we have accumulated matched ensembles on a coarse $8^3 \times 16$ lattice with $a = 0.229(3)\text{fm}$ [1] and a finer $12^3 \times 24$ lattice with $a = 0.178(6)\text{fm}$ [2], with scale set by assuming the two color string tension is $(440\text{MeV})^2$. Both lattices have temperature $T \approx 50\text{MeV}$, making them “cold” in QCD terms. The quark mass is relatively heavy, corresponding to $m_\pi/m_\rho \approx 0.8$ — up to now we have not considered the chiral limit to be so important, because effects due to $m \neq 0$ could naively be expected to lie deep at the bottom of the Fermi Sea. In our most recent simulations [3] we have explored the systematics both of varying the diquark source $ja = 0.04, \dots, 0.02$ and varying T , with $N_\tau = 24, \dots, 8$ corresponding to $T = 47, \dots, 141\text{MeV}$.

3. Equation of State

Fig. 2 plots n_q/n_q^{SB} as a function of μa , calculated on the fine lattice with $ja = 0.04$ [2]. Here n_q^{SB} denotes the “Stefan-Boltzmann” (SB) result evaluated for free Wilson fermions on the same volume; taking the ratio is a first step towards correcting for discretisation and finite volume artifacts. These are considerable, as shown by the departures from unity in Fig. 5. For μa greater than unity, the dominant error is due to UV artifacts, but for smaller μ the disparity between the two curves points to the IR; indeed, the oscillatory behaviour is due to departures of the Fermi surface from sphericity as $T \rightarrow 0$ due to the discretisation of momentum space [4]. Fig. 3 illustrates the difficulty of disentangling these two effects, updating Fig. 2 for a range of temperatures with the limit $j \rightarrow 0$ taken. Fig. 4 presents the same data normalised by the continuum SB result $N_f N_c (\mu^3/\pi^2 + \mu T^2)/3$. The apparent peak at $\mu a \approx 0.4$, previously identified as a signal of Bose-Einstein condensation (BEC) of tightly bound diquarks [1, 2], is most likely an IR artifact due to the dip in the dashed red free fermion curve of Fig. 5. On the other hand the difference in vertical scales shows that UV artifacts still need to be corrected.

Another previously neglected factor is the $j \rightarrow 0$ limit, which appears to be a much more important effect for interacting quarks; setting $j \neq 0$ enhances their tendency to form pairs, in effect promoting BEC formation which could deform the results. Taking all factors into account, we conclude the approximate plateau in the range $0.4 < \mu a < 0.7$ is consistent with $n_q/n_q^{SB} \approx 1$, rather than 1.4 as suggested by Fig. 2. The same gross features are also apparent in a calculation of the pressure $p = \int^\mu n_q d\mu$; Fig. 6 shows the result of three different approaches to correcting for lattice artifacts at $T = 47\text{MeV}$ [3].

Figs. 3, 4 and 6 support an interpretation in terms of four distinct regimes separated by three

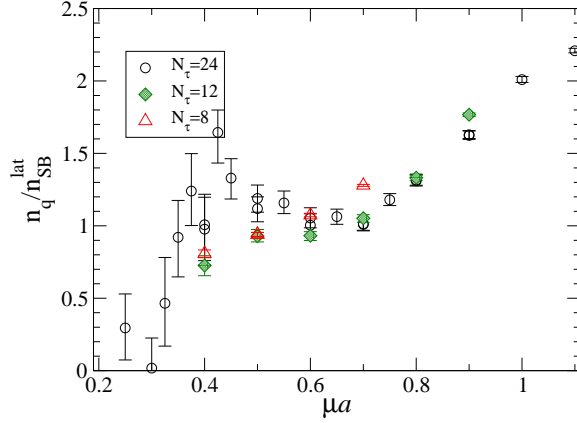


Figure 3. n_q/n_q^{SB} for $j \rightarrow 0$ using lattice free fermions.

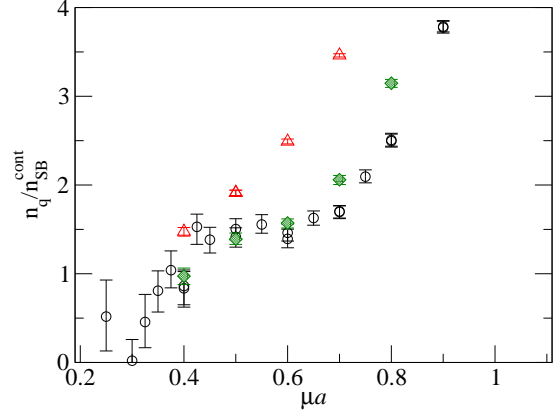


Figure 4. n_q/n_q^{SB} for $j \rightarrow 0$ using continuum free fermions.

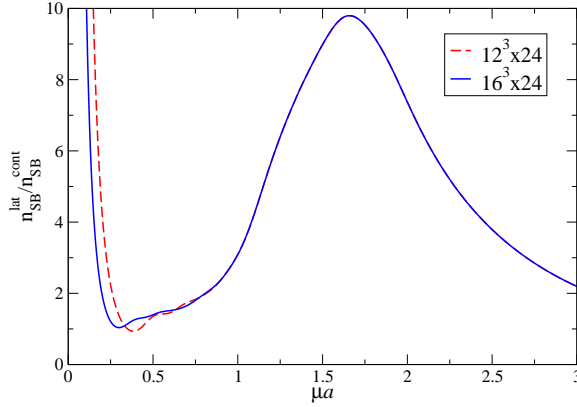


Figure 5. $3\pi^2 n_q^{SB}/N_f N_c \mu^3$ vs. μa on two different lattice volumes.

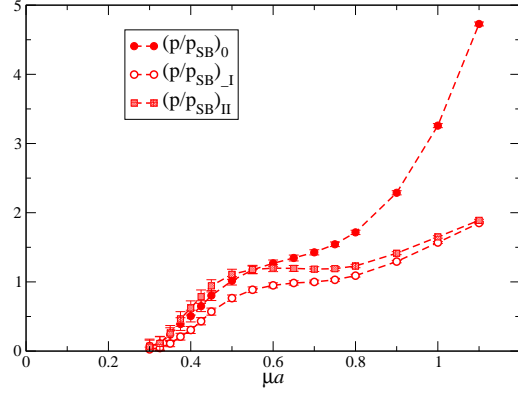


Figure 6. p/p^{SB} on $12^3 \times 24$ for $j \rightarrow 0$ using three different artifact correction schemes.

thresholds. The first is the onset threshold, taking place at $\mu_o = m_\pi/2 \approx 0.32a^{-1} \approx 360\text{MeV}$, separating the vacuum state from a non-zero quark density $n_q > 0$. In mean field theory this is predicted to be a second order phase transition [5], unlike the first order transition expected in QCD. The non-monotonic behaviour of n_q/n_q^{SB} above onset due to a BEC, predicted in mean field-theory, and reported in [1, 2] is, however, no longer a robust feature of the numerical results; it may well be that simulations far closer to the chiral limit are needed to expose this behaviour. Next, at $\mu_Q \approx 0.5a^{-1} \approx 530\text{MeV}$ is a crossover to a régime where both n_q and p are approximately equal to their SB values, suggestive that a degenerate system of quarks with a well-defined Fermi momentum $k_F \propto n_q^{1/3}$ and Fermi energy $E_F \approx \mu$ has formed. For reasons that will be elaborated we refer to this as the *quarkyonic* régime. Finally at $\mu_d \approx 0.8a^{-1} \approx 850\text{MeV}$ both n_q and p start to climb above the SB values. If for the moment we assume the degenerate quark description still holds, then for $\mu_Q < \mu < \mu_d$ we have $E_F \approx k_F$ as expected for weakly interacting massless quarks, but $E_F < k_F$ for $\mu > \mu_d$, implying that the quark matter at very large densities has a large negative correction to the kinetic energy, ie. it is strongly self-bound.

4. Order Parameters and Phase Diagram

In order to characterise the high density system we have also examined two “order parameters”, one exact, the other approximate. Fig. 7 shows the superfluid order parameter $\langle qq \rangle$ as a

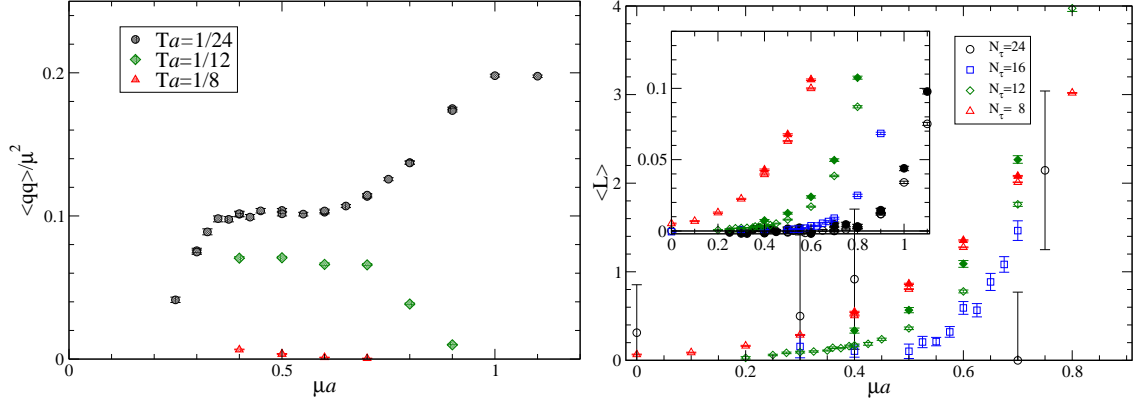


Figure 7. $\langle qq \rangle / \mu^2$ for $j \rightarrow 0$ for various T . **Figure 8.** Polyakov line $L(\mu)$ for various T .

function of μ , extrapolated to $j = 0$, for three different temperatures. For a degenerate system superfluidity arises through Cooper pair condensation of diquark pairs at the Fermi surface; hence $\langle qq \rangle$ should scale as the area of the Fermi surface k_F^2 . The plot shows $\langle qq \rangle / \mu^2$, and indeed it is remarkably constant within the quarkyonic régime, although clearly T -sensitive. The temperature sensitivity becomes more marked once $\mu > \mu_d$, and at the highest temperature studied the order parameter vanishes everywhere, implying restoration of the “normal” phase.

We also studied the Polyakov loop L as a function of both μ and T . Since this involves comparison of data with different N_τ , it has been necessary to renormalise L via multiplication by a factor $Z_L^{N_\tau}$ [6], determined at $\mu = 0$ and normalised so that $L(T = 1/4a) \equiv 1$. The results are shown in Fig. 8; the inset shows the unrenormalised data. First consider the data from the lowest temperature with $N_\tau = 24$. Although in the presence of fundamental matter L is not an exact order parameter for global Z_{N_c} center symmetry, its behaviour strongly suggests that the transition at μ_d is for all practical purposes identical with deconfinement, ie. the free energy for a static fundamental color source becomes finite once $\mu > \mu_d$. The quark density at deconfinement is $16 - 32 \text{ fm}^{-3}$ (the uncertainty arises from the difficulty in handling lattice artifacts discussed in the previous section), some 30 – 60 times that of nuclear matter.

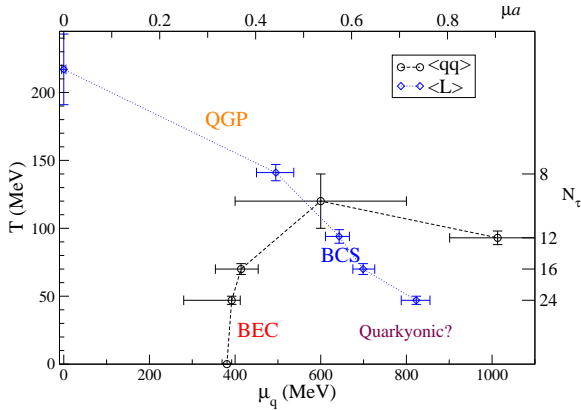


Figure 9. Tentative QC₂D phase diagram.

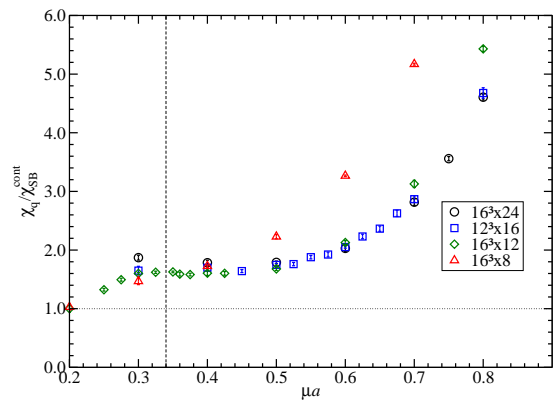


Figure 10. χ_q / χ_q^{SB} for $ja = 0.04$, various T .

It’s then interesting that μ_d defined via L falls rapidly as T rises. A pragmatic definition of $\mu_d(T)$ is the value at which $L(\mu, T) \approx L(0, T_d)$. The resulting tentative phase diagram is shown in Fig. 9. There are at least three distinct regions/phases: a normal hadronic phase with

$\langle qq \rangle = 0$, $L \approx 0$ at low T and μ ; the quarkyonic region with $\langle qq \rangle \propto \mu^2$ and $L \approx 0$ at low T and intermediate μ ; and a deconfined, normal phase with $\langle qq \rangle = 0$, $L > 0$ at large T and/or large μ . At this stage we cannot exclude a deconfined superfluid phase at large μ and small/intermediate T . The “quarkyonic” nomenclature is now justified; this phase has the thermodynamic bulk scaling of a weakly-interacting degenerate quarks, but remains confined. It thus has two of the features of dense baryonic matter originally proposed on the basis of large- N_c arguments [7].

5. Quark Number Susceptibility and Deconfinement

We have also recently calculated the quark number susceptibility $\chi_q \equiv \partial n_q / \partial \mu$ [8, 3]. Whilst naively χ_q is expected to reflect local fluctuations of the n_q operator, it turns out that at large μ the dominant term comes from a connected “hairpin” diagram. Fig. 10 shows χ_q divided by the continuum SB result. Once again, we note a large range over which the ratio is approximately constant; indeed it is compatible with one as $j \rightarrow 0$, though more sensitive to the quark mass value used for the free fermions than other bulk observables [3].

The most striking feature of Fig. 10, however, is the absence of T -dependence at all but the highest temperature studied (141 MeV), is in stark contrast to the behaviour of L in Fig. 8. Despite our intuition from the thermal transition in QCD [9], χ_q cannot be regarded as a proxy for L once $\mu/T \gg 1$. We conjecture that the change in behaviour of the bulk thermodynamic quantities n_q , p and χ_q observed at μ_d is a transition from short-ranged binary confining interactions to longer-ranged interactions among several quarks within the medium, and that this corresponds with the transition from weak to strong self-binding noted in Sec. 3. The T -dependent behaviour of L , in contrast, must be due to degrees of freedom close to the Fermi surface which can be thermally excited; a correlation between gapless excitations and $L > 0$ has also been noted in analytical and numerical studies on small cold volumes [10]. The same phenomenon should inform a theory of transport properties.

6. Summary

QC₂D offers an accessible theoretical laboratory for the study of dense baryonic matter. For low T at least three physical regions can be identified: the vacuum for $\mu < \mu_o$; a confined quarkyonic superfluid for $\mu_Q < \mu < \mu_d$; and a deconfined phase for $\mu > \mu_d$. The most recent simulations have only made our findings in the quarkyonic régime more robust. Not discussed here are new results for renormalised energy density, conformal anomaly, and chiral symmetry restoration [3].

Acknowledgments

This work used the DiRAC Facility jointly funded by STFC, the Large Facilities Capital Fund of BIS and Swansea University. We thank the DEISA Consortium (www.deisa.eu), funded through the EU FP7 project RI-222919, for support within the DEISA Extreme Computing Initiative.

References

- [1] S. Hands, S. Kim and J.-I. Skullerud, *Eur. Phys. J. C* **48** (2006) 193.
- [2] S. Hands, S. Kim and J.-I. Skullerud, *Phys. Rev. D* **81** (2010) 091502(R).
- [3] S. Cotter, P. Giudice, S. Hands and J.-I. Skullerud, *Preprint* arXiv:1210.4496 [hep-lat].
- [4] S. Hands and D.N. Walters, *Phys. Lett. B* **548** (2002) 196.
- [5] J.B. Kogut, M.A. Stephanov, D. Toublan, J.J.M. Verbaarschot and A. Zhitnitsky, *Nucl. Phys. B* **582** (2000) 477.
- [6] S. Borsanyi *et al.*, *Phys. Lett. B* **713** (2012) 342.
- [7] L. McLerran and R.D. Pisarski, *Nucl. Phys. A* **796** (2007) 83.
- [8] P. Giudice, S. Hands and J.-I. Skullerud, *PoS LATTICE* **2011** (2011) 193.
- [9] Y. Aoki, Z. Fodor, S.D. Katz and K.K. Szabo, *Phys. Lett. B* **643** (2006) 46; A. Bazavov *et al.*, *Phys. Rev. D* **80** (2009) 014504.
- [10] S. Hands, T.J. Hollowood and J.C. Myers, *JHEP* **1007** (2010) 086; *JHEP* **1012** (2010) 057.